IEEE Access
Multidisciplinary | Rapid Review | Open Access Journal

Received March 25, 2018, accepted May 17, 2018, date of publication May 23, 2018, date of current version June 19, 2018.

Digital Object Identifier 10.1109/ACCESS.2018.2839737

Virtual Inertia Control Strategy in Microgrid Based on Virtual Synchronous Generator Technology

KAI SHI, HAIHAN YE, WENTAO SONG, AND GUANGLEI ZHOU
School of Electrical and Information Engineering, Jiangsu University, Zhenjiang 212000, China

Corresponding author: Haihan Ye (yehaihan2016@163.com)

This work was supported in part by the National Natural Science Foundation of China under Award 51407085, in part by the Postdoctoral Science Foundation of China under Award 2015M571685, in part by the Priority Academic Program Development of Jiangsu Higher Education Institution, and in part by the Jiangsu University Senior Talents Special Project under Award 13JDG111.

ABSTRACT Although the virtual inertia algorithm can be used to enhance the inertia of microgrid system, the strong coupling and low precision always limit its popularization and application. Therefore, a novel virtual inertia control strategy is proposed in this paper. Combining with the potential inertia advantages of virtual synchronous generator (VSG) technology, the poor compatibility between the virtual inertia principle and the energy storage control algorithm is analyzed in detail. In order to improve the control precision, this paper focuses on the analysis of frequency response characteristics of alternating current (ac) side and then regulates the ac frequency more directly and accurately by the virtual inertia generated from the energy storage device and the grid-connected inverter. Thus, additional droop characteristic, particular control algorithm of energy storage device, and power given module are designed, respectively, to make the system provide virtual inertia power support actively under multi disturbance operation. The novel virtual inertia control strategy can effectively deal with all kinds of wind speed and ac load mutation and restrain the frequency variation on ac side. Finally, the correctness and feasibility of the proposed scheme are verified by the simulation results.

INDEX TERMS Virtual synchronous generator, virtual inertia, energy storage device, frequency stability, microgrid.

I. INTRODUCTION

With the increasing utilization of renewable energy and the extensive access of new loads in recent years, the installation ratio of traditional synchronous generators (SG) in power grid is gradually reduced, which relatively reduces the spinning reserve capacity and the moment of inertia and brings great challenges to the stability of whole microgrid system. In traditional wind power plants, passive adaptive control algorithm is always adopted in grid-connected inverters. Although this kind of control strategy can steady deliver the power obtained by the maximum power point tracking (MPPT) algorithm, the rotor speed and the alternating current (AC) load are completely decoupled, which makes the generator becomes an isolated constant power source. Therefore, traditional grid-connected algorithm, mostly designed for stable operation, has limited contribution to the inertia support in a direct way.

Therefore, improving the stability of the microgrid system and adapting the operating environment under new situation is an important issue for smart grid construction. The virtual inertia in double fed induction generator (DFIG) was analyzed in [1], where the virtual inertia control technology was proposed based on the MPPT optimization. However, the presented scheme in [1] has some demerits including slow response speed and coupling with MPPT algorithm. Besides this, the problem of release speed decline of rotor kinetic energy caused by the inertia moment increment was not analyzed. An integrated control strategy was proposed in [2] to make the system possess both virtual inertia and primary frequency regulation. However, the proposed control strategy requires additional overspeed or deloading methods and pitch angle control algorithm, which causes lower utilization rate of wind energy. Moreover, this scheme

may easily cause the logic chaos in energy storage device when the wind speed and AC load change simultaneously. A variable coefficient combined virtual inertia and primary frequency control strategy for DFIG is proposed in [3], the influence of droop control gain setting was analyzed under different wind speeds to realize the variable coefficient method. The influence of PLL on virtual inertial control is analyzed deeply in [4]. It shows that the smaller the PI parameters of PLL are, the bigger the electromechanical oscillation mode damping ratio is.

In recent years, some scholars put forward the virtual synchronous generator (VSG) technology [5]–[7]. This novel technology introduces the basic theory and operation experience of SG into the design of grid connected algorithm, and effectively resolves the problems of low damping and inertia [8]–[10]. At present, the problems of VSG technology such as parallel operation in power grid [11]–[13], application of energy storage device [14], [15], inertia adaptive control strategy [16]–[19] were researched extensively, and some corresponding results were obtained. In [20], the small-signal model of the grid-connected converter is established to deduce the dynamic characteristic of the dc bus voltage with power fluctuation. However, this scheme does not involve the contribution of energy storage devices and grid-connected inverter to the virtual inertia.

Based on the VSG technology employed as the grid-connected algorithm, it helps to make the grid-connected inverter equivalent to be a synchronous generator, which can make the system much closer to the theory analysis conditions of traditional virtual inertia algorithm. The potential inertia advantage of VSG technology also can be used to actively regulate frequency. Besides, this paper focuses on the analysis of the frequency response characteristics of AC side, and then regulates the AC frequency more directly and accurately by the virtual inertia generated from both the energy storage device and the grid-connected inverter. With the rapid response of power electronic equipment, the slow kinetic energy conversion speed of the traditional virtual inertia algorithm is improved. When wind speed and AC load mutates at the same time, the frequency of AC side can be adjusted effectively, and the operating characteristics of other control algorithms in microgrid remain unchanged.

Section 2 is used to analyze the traditional virtual inertia algorithm, and point out the basic problems of that. Section 3.1 introduces the basic composition and potential advantages of VSG, which is the important theoretical basis of almost all work in this paper. Section 3.2 shows the poor compatibility between the virtual inertia principle and the energy storage control algorithm when VSG is employed. Section 4 is the specific design method of the proposed control method. In section 5, this control strategy is verified by Matlab/simulink platform under two cases. One case is the AC load mutation, and the other is the simultaneous mutation of wind speed and AC load. Finally, the conclusion is given in section 6.

II. RESPONSE ANALYSIS OF TRADITIONAL VIRTUAL INERTIA CONTROL ALGORITHM

A. THE STRUCTURE OF TRADITIONAL MICROGRID SYSTEM

As shown in Fig. 1, the traditional microgrid structure includes generator, energy storage device, DC bus, SG, AC load and inverters. Most of traditional grid-connected inverters adopt P/Q type algorithm to transmit power, but that cannot stabilize the voltage of AC load. Therefore, a SG is required at the side of AC load [1], [2].

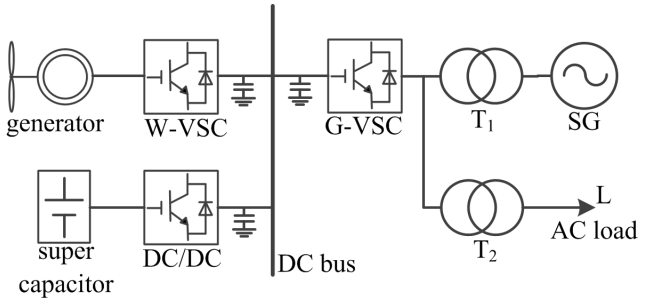

FIGURE 1. Block diagram of microgrid.

When the MPPT algorithm is adopted, the output power of the generator is only related to wind speed, where the generator can be approximated to a constant power source. When AC load increases substantially, the generator hardly produces additional response. Thus, all of the power increment of the AC load is undertaken by the SG or the power grid. That is, the generator has limited contribution to the frequency regulation of the AC side, and the stability of microgrid mainly depends on the stability of SG or power grid. Therefore, the lack of inertia capability in microgrid system may endanger the stability of SG and power grid.

B. BASIC PRINCIPLE OF VIRTUAL INERTIA

In order to enhance the inertia supporting capability of microgrid system, the virtual inertia technology is proposed based on the MPPT optimization [1]. The schematic diagram is shown in Fig. 2, where n_r is the mechanical speed of the generator.

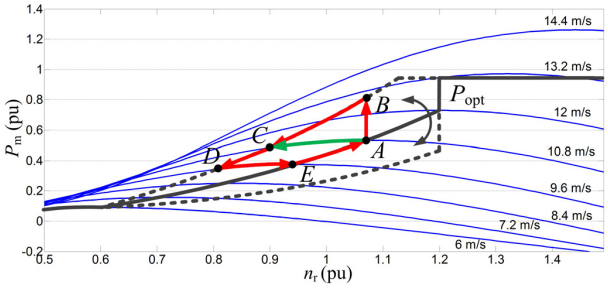

FIGURE 2. Schematic diagram of virtual inertia technology based on MPPT optimization.

When the microgrid system is stable, the generator runs at point A. When the AC load substantially increases,

the generator jumps from point A to point B in CB saturation curve by using the wind energy utilization coefficient. At this moment, the output electromagnetic power of the generator is more than input mechanical power, and the transient adjustment of rotor speed begins. When the generator operation passes through point C, the electromagnetic power at point C is approximately equal to that at point A, but the rotor speed has a decrease of |AC| horizontal component. Thus, a large amount of kinetic energy has been released during the transient process, as shown in the green arrow in Fig. 2.

When the mechanical torque is balanced with the load torque, the rotor speed tends to be stable. At this time, the transient process finishes, and the rotor kinetic energy is released completely. After that, the MPPT algorithm is used to restore the steady-state output power by making the generator operate along the curve D-E-A to point A finally. Thus, it can be seen that the rotor kinetic energy of the generator can provide transient frequency support when the AC load changes.

C. THE ANALYSIS OF TRADITIONAL VIRTUAL INERTIA CONTROL ALGORITHM

According to rotor equation of SG,

$$T_{\mathrm{m}} - T_{\mathrm{e}} = J_{\mathrm{g}} \frac{d\omega_{\mathrm{r}}}{dt}. \tag{1}$$

where T_{m} is the input mechanical torque, T_{e} is the output electromagnetic torque, J_{g} is the moment of inertia of SG, ω_{r} is the mechanical angular speed.

If T_{m} keeps constant and J_{g} increases in (1), the magnitude of the speed change caused by AC load mutation will be much smaller. This also means that the frequency deviation magnitude of the AC side will be smaller when SG is directly connected to the AC load.

According to the expression of rotor kinetic energy,

$$E_{\mathrm{k}} = \int (P_{\mathrm{m}} - P_{\mathrm{e}})dt = \int J_{\mathrm{g}}\omega_{\mathrm{r}} d\omega_{\mathrm{r}} = \frac{1}{2} J_{\mathrm{g}} \omega_{\mathrm{r}}^2. \tag{2}$$

where P_{m} is the input mechanical power, P_{e} is the output electromagnetic power.

And then, the variation of rotor kinetic energy can be calculated

$$\Delta E_{\mathrm{k}} = \frac{1}{2} J_{\mathrm{g}} [(\omega_{\mathrm{r}} + \Delta\omega)^2 - \omega_{\mathrm{r}}^2]. \tag{3}$$

Because of the relatively slow response of mechanical speed, the following equation can be obtained by substituting (1) into (3) with differential form,

$$\Delta E_{\mathrm{k}} = \frac{(T_{\mathrm{m}} - T_{\mathrm{e}})^2}{2J_{\mathrm{g}}} (\Delta t)^2 + (T_{\mathrm{m}} - T_{\mathrm{e}}) \Delta t \omega_{\mathrm{r}}. \tag{4}$$

It shows that the less kinetic energy is released in the same time if J_{g} increases, which results in the low release rate and conversion efficiency of the rotor kinetic energy. This conflicts with the immediacy of the AC load mutation, and the unbalanced power in microgrid still brings heavy burden to SG or power grid. Therefore, virtual inertia not means to merely increase the equivalent moment of inertia, or just learn from the rotor inertia principle of SG. The virtual inertia control algorithm should be able to provide required inertial support to the system more actively and directly.

The traditional virtual inertia algorithm can effectively provide frequency support, but it can only assist the SG or power grid to offset the power difference in the transient process. Because the saturation curve of MPPT is difficult to be accurately calculated, the unbalanced power cannot be completely suppressed, and the transient impact and concussion of the system is difficult to avoid. Moreover, the virtual inertia algorithm above requires additional overspeed or deloading methods and pitch angle control algorithm, which causes complex control structures and lower utilization rate of wind energy. If the AC load mutates during the change of wind speed, the logical judgment of the system is prone to confusion, resulting in the delay or misoperation of the energy storage device.

III. NOVEL VIRTUAL INERTIA CONTROL ALGORITHM BASED ON VSG

A. BASIC PRINCIPLE OF VSG TECHNOLOGY

The classic topology of VSG is shown in Fig. 3, where u_{dc} and i_{dc} are voltage and current of the DC bus, L_{s}, R_{s}, C are parameters of LCL filter, i_{gk} is the current of k phase.

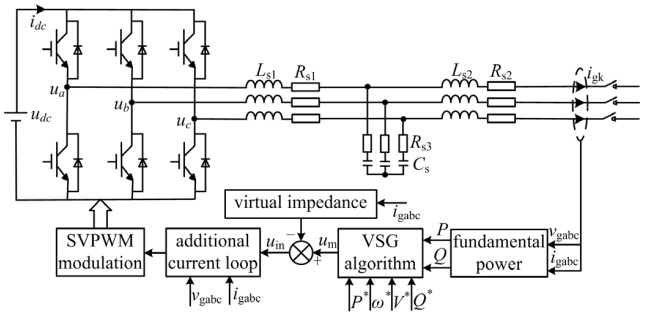

FIGURE 3. Block diagram of VSG topology.

As shown in Fig. 3, three phase voltage signal um is obtained by the output active and reactive power of LCL filter and droop characteristics of VSG algorithm, which are used to simulate the operation characteristics of SG. After modulated by the virtual impedance and the additional current loop, this modulated wave is sent to space vector pulse width modulation (SVPWM) module to drive the grid-connected inverter. Thus, this distributed power source can be equivalent to a SG.

The mathematical model of the VSG algorithm module in Fig. 3 can be described as

$$\begin{cases} P^* + D_{\mathrm{p}}(\omega^* - \omega) - P = J\omega^* \dfrac{d\omega}{dt} \\ Q^* + D_{\mathrm{q}}(V^* - V) - Q = K \dfrac{dE}{dt} \\ \theta = \displaystyle\int \omega dt. \end{cases} \tag{5}$$

where P^* and Q^* are given active and reactive power, D_p and D_q are P-f and Q-V droop coefficients, P and Q are feedback value of active and reactive power, J and K are the inertia coefficients of active and reactive power loops, ω^* and ω are rated angular velocity and virtual rotor angular velocity, V^* and V are rated voltage amplitude and output voltage amplitude, E is the potential of VSG, and θ is virtual rotor position angle.

Equation (5) shows that VSG technology is designed to simulate the operating characteristics of SG. Thus, VSG technology helps to make the grid-connected inverter here equivalent to be a SG, which can make the system much closer to the theory analysis of traditional virtual inertia algorithm.

When AC load increases suddenly, ω droops and the droop characteristic instantaneously produces a positive power increment to offset the power increment of AC load, which helps to restrain further descent of ω. When the frequency drops to a steady value, the system becomes stable and automatically balances the power difference. Thus, it can be seen that VSG itself has excellent ability of inertia and primary frequency regulation, which helps to design new virtual inertia control algorithms.

B. THE COMPATIBILITY ANALYSIS OF VIRTUAL INERTIA AND ENERGY STORAGE ALGORITHM

After adopting the principle of virtual inertia, the control algorithm of energy storage device should be specially designed so that the function of energy storage and virtual inertial support can be achieved simultaneously. As shown in Fig. 4, the virtual inertia algorithm in the energy storage device also tries to adopt the double-loop structure to improve its compatibility and reliability.

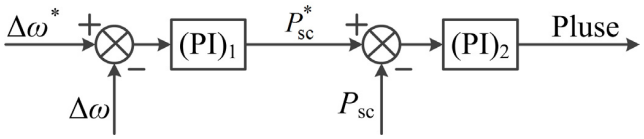

FIGURE 4. Double-loop structure diagram of virtual inertia control algorithm in energy storage.

When the AC load mutation occurs, the unbalanced power triggers the droop characteristics in VSG and the virtual inertia in energy storage device simultaneously. This can be expressed by the following equation,

$$\Delta P = D_p \Delta\omega + P_{sc}(\Delta\omega). \tag{6}$$

where, P_{sc} is the output power of super capacitor.

By ignoring the integral part of the PI first, the performance of above virtual inertia algorithm is studied in the following. According to the outer loop,

$$P_{sc}(\Delta\omega)^* = (\mathrm{PI})_1(\Delta\omega^* - \Delta\omega) \approx k_1(\Delta\omega^* - \Delta\omega). \tag{7}$$

where, k_1 is the proportional coefficient of $(\mathrm{PI})_1$.

By substituting (7) into (6), it can be obtained,

$$\Delta P = D_p \Delta\omega + k_1(\Delta\omega^* - \Delta\omega). \tag{8}$$

And then, (8) can be simplified as follows,

$$\Delta\omega = \frac{\Delta P - k_1 \Delta\omega^*}{D_p - k_1}. \tag{9}$$

Because $\Delta\omega$ and $k_1\Delta\omega^*$ are far less than ΔP, the constraints shown in (9) can be simplified to as follows,

$$\Delta P \ll (D_p - k_1). \tag{10}$$

Based on the coefficient of P-f droop characteristic,

$$D_p = \frac{\Delta P_{max}}{\Delta\omega_{max}}. \tag{11}$$

where ΔP_{max} is the maximum adjustment range of active power, $\Delta\omega_{max}$ is the maximum fluctuation range of electrical angular velocity.

Constraint condition (10) can be simplified with (11),

$$\Delta P \approx 0.1 \times \left(\frac{\Delta P_{max}}{\Delta\omega_{max}} - k_1\right). \tag{12}$$

Since ΔP is far bigger than $0.1P_{max}/\Delta\omega_{max}$, ΔP is almost positively related to $-0.1k_1$, which means that proportional coefficient of $(\mathrm{PI})_1$ should be very large to meet the design requirements. However, the excessive proportional coefficient can easily cause system shock, and even exceed the stability range of microgrid system. Therefore, the additional performance of energy storage algorithm cannot achieve the desired control target by using the double loop structure with input $\Delta\omega_{max}$.

Specially, when k_1 takes $-k'D_p$, (9) can be simplified as

$$\Delta\omega = \frac{\Delta P + k' D_p \Delta\omega^*}{(k'+1)D_p} \approx \frac{\Delta P}{(k'+1)D_p} = \frac{\Delta\omega'}{(k'+1)}. \tag{13}$$

where $\Delta\omega'$ is the difference of electrical angular velocity when unbalanced power is totally undertaken by VSG droop characteristics.

In (13), when k_1 takes the negative multiples of D_p, the frequency variation amplitude of AC load decreases approximately in the inverse proportion to k', rather than following with $\Delta\omega^*$.

If the control structure shown in Fig. 4 is changed to be hysteresis control method, the system can only work near the rated working frequency. When VSG produces droop characteristics, $\Delta\omega$ turns to be positive or negative all the time. That is, half of switches in the DC/DC converter always stay open, and the other switches continue to be shut down, so the energy storage device doesn't work properly. It can be seen that the hysteresis control method here will cause the VSG to lose its droop characteristics and aggravate the power imbalance in the main circuit.

IV. NOVEL VIRTUAL INERTIA CONTROL STRATEGY

A. MAIN IDEAS

The main design objective of this virtual control strategy is to reasonably use the hidden energy of microgrid to reduce the burden of SG or power grid, and to improve the autonomic regulation ability without sacrificing the performance of other original control algorithm in microgrid system, when wind speed or AC load changes.

Therefore, based on the potential advantages of VSG inertia response, the following basic ideas are proposed:

(1) The rapid response of VSG inertia is applied to quickly use the rotor kinetic energy of the generator, and improve the transient performance. By setting an appropriate adjustment range, the variation range of rotation speed and torque can be restricted to avoid runaway or shut down.

(2) With the droop characteristic of VSG, the energy contained in the energy storage device is fully used to enhance the steady-state performance.

(3) The virtual inertia control algorithm is designed to be independent of other original algorithm, such as energy storage algorithm, MPPT algorithm, the generator control algorithm and VSG algorithm. These algorithms work together to contribute to the overall operation control of ''power grid friendly'' wind power plant.

(4) The frequency of AC side should be regulated more directly and accurately. The traditional virtual inertia control algorithm focuses on the analysis of equivalent rotational inertia of the generator, and then estimates the transient output power indirectly. However, this paper focuses on the analysis of the frequency response characteristics of AC side, and then regulates the AC frequency more directly and accurately by the virtual inertia generated from the energy storage device and the grid-connected inverter.

(5) A unified virtual inertia control strategy is desired, which can be applied for all types of generators. Among them, VSG technology can be used to make the system much closer to the theory analysis conditions of traditional virtual inertia algorithm.

B. ADDITIONAL DROOP CHARACTERISTIC

According to the basic principle of traditional virtual inertia control algorithm, the corresponding analysis is applied to the microgrid system based on VSG technology. Instead of employing additional overspeed or deloading methods and calculating the saturation curve, a threshold is set in the energy storage device so that the generator provides virtual inertial support within the threshold range.

When AC load changes, the generator produces transient power support because of the inertia of rotor speed and the instantaneity of torque. With the decrease of the rotor speed, the generator releases kinetic energy and promotes the transient power balance. By setting the appropriate threshold, the variation range of speed or torque will be limited to ensure that the generator does not runaway or shut down.

Furthermore, additional droop characteristics are designed to adjust the droop characteristics of VSG, which also helps to promote the parallel operation of multiple machines. In Fig. 5, ΔP_{gmax} and $\Delta\omega_{\mathrm{gmax}}$ are the setting range of additional droop characteristics to design the power increment coefficient $k_{\Delta\mathrm{P}}$.

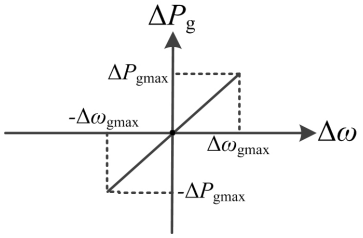

FIGURE 5. Additional droop characteristic.

The additional droop characteristic shown in Fig.5 is

$$\Delta P_{\mathrm{g}} = \frac{k_{\Delta P}}{\Delta\omega_{\mathrm{gmax}}} P^* \times \Delta\omega. \tag{14}$$

By substituting the additional droop characteristic into VSG active power loop,

$$P^*\left(1 + \frac{k_{\Delta\mathrm{P}}}{\Delta\omega_{\mathrm{gmax}}} \times \Delta\omega\right) + D_{\mathrm{p}}(\omega^* - \omega) - P = J\omega^*\frac{d\omega}{dt}. \tag{15}$$

Equation (15) can be simplified as

$$P^* + \left(\frac{k_{\Delta\mathrm{P}}P^*}{\Delta\omega_{\mathrm{gmax}}} + D_{\mathrm{p}}\right) \times \Delta\omega - P = J\omega^*\frac{d\omega}{dt}. \tag{16}$$

Therefore, the additional droop characteristic just enhances the equivalent P-f droop coefficient of VSG active power loop, which does not interfere with VSG operation. For the same magnitude of power difference, the larger the equivalent coefficient of droop characteristic is, the smaller is the frequency difference $\Delta\omega$, which conforms to the SG regulation experience. It can be seen that this method is helpful to adjust the droop characteristics of VSG and unify the droop response characteristics in microgrid.

Because the proposed control strategy does not exist in the inverter after the generator, the MPPT algorithm and the generator control algorithm still play a major role in the wind turbine and the generator. Because they are not the main research work of this paper, it is not discussed in detail here.

C. PARTICULAR CONTROL ALGORITHM OF ENERGY STORAGE DEVICE

The energy storage device is mainly used to maintain the power balance in the main circuit. Both of energy storage algorithm and virtual inertia algorithm are absorbing or releasing energy to reduce the negative impact of unbalanced power in microgrid.

When the AC load increases, the feedback power P increases suddenly. At this time, the generator and the energy storage device provide power support together to maintain power balance. However, according to the active power loop,

$$P^* + D_{\mathrm{p}}(\omega^* - \omega) - P = J\omega^*\frac{d\omega}{dt}. \tag{17}$$

It can be seen that P^* in (17) only means the power delivered by the generator, the power delivered by energy storage device is not included. That is, the virtual power increment $D_p(\omega^* - \omega)$ is generated according to P^* and P, and then droop characteristics is produced by VSG.

Combining with MPPT, energy storage device and the additional droop characteristics, (17) can be reduced as

$$P_m \times \eta_g + P_{sc} + D_p(\omega^* - \omega) - P = J\omega^* \frac{d\omega}{dt}. \quad (18)$$

where η_g is the rated efficiency of the generator.

At the same time, the active power loop of VSG can accurately express the power of the main circuit. Whether the wind speed mutation, AC load mutation, or mutation of wind speed and AC load at the same time, energy storage device and virtual power of VSG will automatically offset the power difference. Therefore, the energy storage device can not only promote the power balance in main circuit, but also effectively adjust the droop characteristics of VSG by using the power stored in it. Combining with the additional droop characteristics mentioned above, the flexible regulation of VSG droop characteristics and virtual inertia can be realized.

According to the above analysis, the particular control algorithm of energy storage device is shown in Fig. 6.

In order to participate in the power balance of the main circuit more actively and directly, the control strategy of energy storage device uses a current loop with input information of power. A threshold value is set at the low pass filter (LPF) so that the transient power support of the generator is stable within the threshold so as to avoid runaway or stop. Due to the fact that wind speed is not a sharp-change value, wind speed variation has limited influence on VSG stability when the generator operates in the threshold range.

Since the energy storage device operates in a large disturbance environment with very fast response speed, the design of energy storage device control algorithm should have high reliability. Switch 1 and Switch 2 are used to shield the calculation of operating mode on another mode. Switch 3 is used to shield the influence of VSG calculation on the control algorithm when energy storage device is not accessed. Switch 4 is used to output the control signals of operating mode individually. $u_{sc} + 10^{-9}$ is used to prevent computation errors when the denominator drops to 0.

If AC load increases substantially when the energy storage device is charging, the energy required is much more than the power obtained by wind power. At this point, ΔP becomes positive to make the control algorithm switches to boost mode, so energy storage device begins to provide the corresponding power support for microgrid. Furthermore, the previous mode does not affect the current operating mode, and the energy storage device can quickly and steadily switch between buck and boost mode.

D. POWER GIVEN MODULE

Specially designed power given module can effectively control the AC side frequency under large disturbance by flexibly regulating P_{set} in the VSG active loop. If $\Delta\omega$ is used as reference value, the power given module will be coupled with the VSG based on above theoretical analysis, so it is difficult to realize the accurately control of AC side frequency. Therefore, the principle of hysteresis control with high reliability is adopted in the proposed scheme.

In the stage of VSG startup and pre-synchronization, P_{set} is set to $P_m\eta_g$. When the VSG runs steady, $|\Delta\omega|$ and $|\Delta\omega^*|$ are compared in real time. If $|\Delta\omega|$ is larger than $|\Delta\omega^*|$, P_{set} is set to $P_m\eta_g + P_{sc}$. At this time, the power difference of main circuit can be used to automatically regulate VSG droop characteristics to ensure the voltage stability of AC side. If $|\Delta\omega|$ is not larger than $|\Delta\omega^*|$, P_{set} is set to $P_m\eta_g + \Delta P_g$ to regulate the steady droop characteristics of the VSG.

In summary, the overall schematic diagram of the proposed control strategy shows bellow.

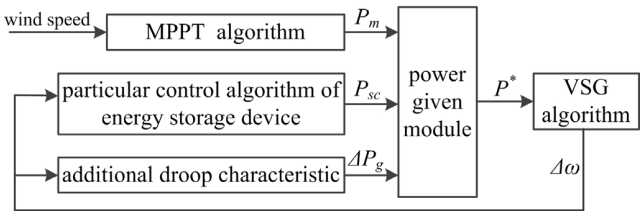

FIGURE 7. overall schematic diagram of the proposed control strategy.

V. THE ANALYSIS OF SIMULATIONS

The simulation model is built in Matlab/simulink platform to verify the above theoretical analysis and the proposed control strategy. The main simulation parameters are shown in Table 1.

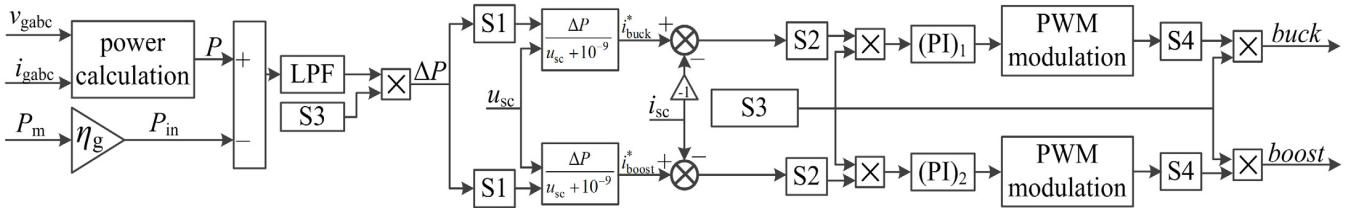

FIGURE 6. Schematic diagram of energy storage device control algorithm.

TABLE 1. Simulation parameters.

Parameter	Value
DC bus voltage (U_{dc})	600 V
First inductance of LCL (L_{s1})	3.2 mH
Capacitance of LCL (C_2)	10 μF
Second inductance of LCL (L_{s3})	0.8 mH
P-f droop coefficient (D_p)	1590
Inertia coefficient of active power loop (J)	0.058 kg·m^2
Q-V droop coefficient (D_q)	320
Inertia coefficient of reactive power loop (K)	6.5 A·s
Capacitance of super capacitor (C_{sc})	12.5 F
Initial voltage of super capacitor (U_{sc0})	80 V
Equivalent resistance of super capacitor (R_{sc})	0.28 Ω
Wind energy utilization coefficient (C_p)	0.34
Swept area of the wind turbine (A)	13.6 m^2
The impeller diameter of the wind turbine (R)	3.4 m
Air density (ρ)	1.25 kg/m^3
Generator efficiency (η_g)	0.7731
Given active power (P^*)	5 kW
switching frequency	10 kHz

A. PERFORMANCE VERIFICATION UNDER AC LOAD MUTATION

About 3.6s, the voltage of DC bus is built up. At 4s, VSG is accessed with no load operation. And then, wind speed increases and AC load is accessed in 5.5s. At 6s, energy storage device is accessed. At 11s, AC load increases by 1 kW. $\Delta\omega^*$ is set to 0 in this simulation.

Fig. 8(a) is the simulation result without adding the proposed control strategy. It can be seen that ω drops to 313.53 after the increase of AC load. Fig. 8(b), 8(c) and 8(d) are the simulation results of proposed control strategy for microgrid system based on VSG technology. In Fig. 8(b), dual stator-winding induction generator [21] is used to test the universality of the proposed control algorithm. 0-4s is no-load voltage build up process for the selected generator. 4-5.5s is pre-synchronization process of VSG. After accessing energy storage device and load starting process, system enters into stable with constant wind speed and constant AC load about 9s. At 11s AC load increases, the rotor speed of generator decreases within the limited variation range and can enter into stable state rapidly. As shown in Fig. 8(c), the frequency of the AC side remains 100×pi, which achieves the control objective. In Fig. 8(d), energy storage device automatically releases 1kW power with small fluctuation. It can be seen that the energy storage device can not only promote the power balance of the main circuit, but also can be used to regulate the output droop characteristics, which conforms to theoretical expectations.

B. PERFORMANCE VALIDATION UNDER THE MUTATION OF WIND SPEED AND AC LOAD

The performance of the proposed virtual inertia control strategy is further verified here. Basically similar to the above simulation conditions, wind speed increases by 0.5 m/s at 11s while AC load increases by 3kW at same time. $\Delta\omega^*$ is set to 2×pi×0.2 in this simulation.

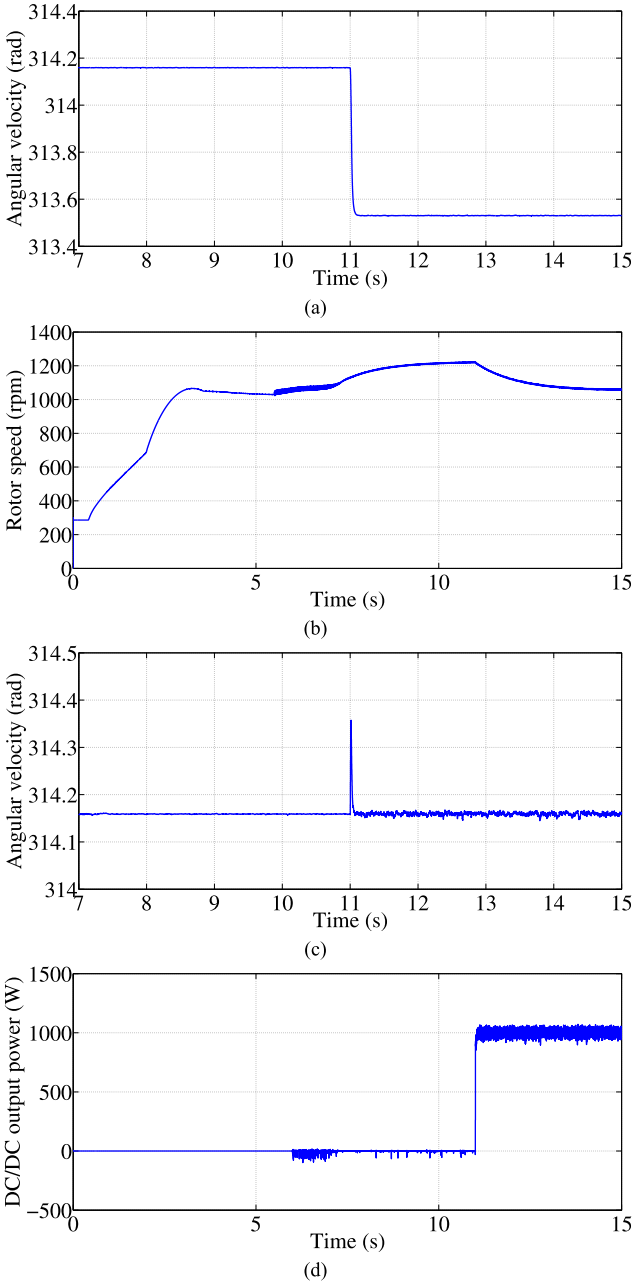

FIGURE 8. Simulation results of AC load mutation: (a) Electrical angular velocity of AC side without proposed control strategy; (b) Rotor speed of the generator; (c) Electrical angular velocity of AC side with proposed control strategy; (d) Output power of energy storage device.

Fig. 9 is the simulation results of virtual inertia control strategy under complex operation environment. In the vicinity of 11s, energy storage device does not work, and the generator operates within the threshold range. At this point, the mutation of wind speed makes the VSG output frequency generate an upward wave crest, which conforms to the theoretical analysis. Calculated from the parameters in Table 1, wind speed increase by 0.5m/s can generate power increment 595.5744W, and thus energy storage device should release 2404.4256W during the steady state. As shown in Fig. 9(a),

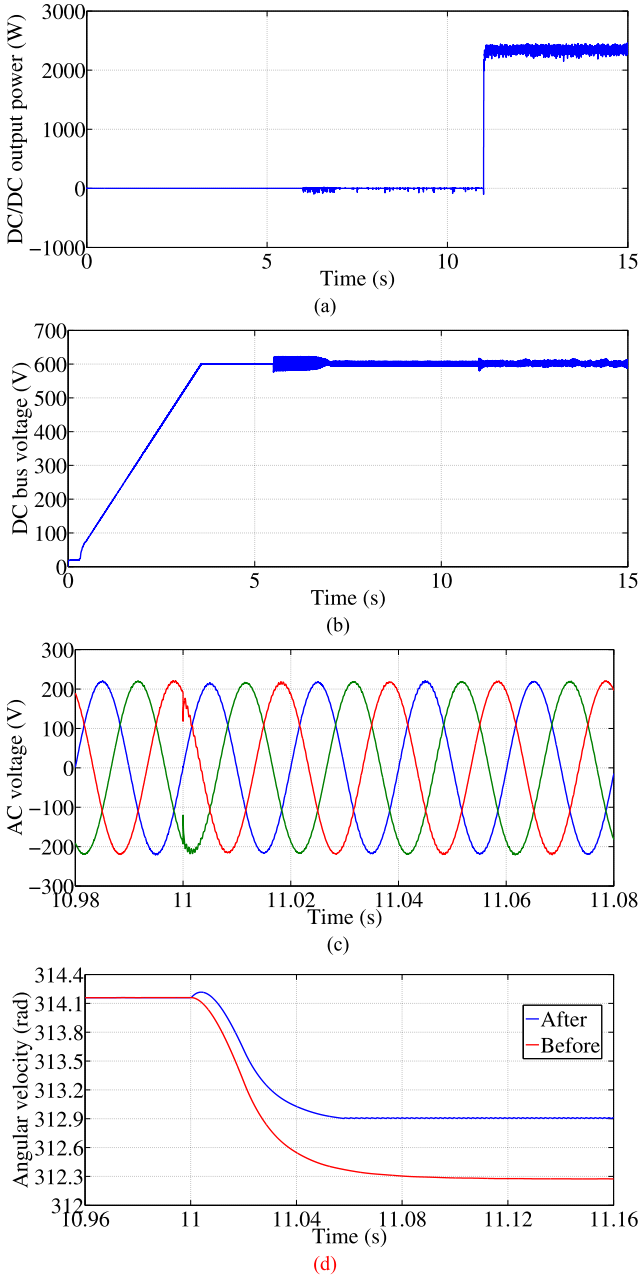

FIGURE 9. Simulation results of simultaneous mutation of wind speed and AC load: (a) Output power of energy storage device; (b) DC bus voltage; (c) voltage waveform of AC side; (d) Electrical angular velocity of AC side.

energy storage device outputs the corresponding power automatically at 11s, which does not cause logic chaos under complex operation environment. In Fig. 9(b), DC side of the system is stable, and the DC bus voltage has good robustness. As shown in Fig. 9(c), the bus voltage remains stable and the AC side voltage has good sine degree. Fig. 9(d) shows that the output frequency can be effectively controlled at ω^*-$\Delta\omega^*$ when the proposed control strategy is added. The adjustment speed and stability of the output frequency have been improved. However, by introducing the mechanical power into the power given module, a slight overshoot of the output frequency is raised due to the wind mutation.

VI. CONCLUSION

In this paper, a novel virtual inertia control strategy is proposed. The potential inertia advantages of VSG are used into the virtual inertia problem, which helps the system much closer to the theory analysis conditions of traditional virtual inertia algorithm. Based on the detailed analysis of the frequency operation characteristics of AC side, additional droop characteristic, particular control algorithm of energy storage device and power given module are designed respectively to improve the initiative and directness of the virtual inertia algorithm. The simulation results prove that this scheme can effectively deal with the mutation of wind speed and AC load, and can improve adjustment speed and accuracy of the output frequency. Besides, both the transient and steady state performance of inertia response in microgrid is improved, which helps to expand the contribution of wind power plants to the stability and frequency regulation of power grid.

REFERENCES

[1] L. Heming, Z. Xiangyu, W. Yi, and X. Zhu, "Virtual inertia control of DFIG-based wind turbines based on the optimal power tracking," *Proc. Chin. Soc. Elect. Eng.*, vol. 32, no. 7, pp. 32–39, 2012.

[2] Y. Fu, Y. Wang, and X. Zhang, "Integrated wind turbine controller with virtual inertia and primary frequency responses for grid dynamic frequency support," *IET Renew. Power Gen.*, vol. 11, no. 8, pp. 1129–1137, 2017.

[3] J. Zhao, X. Lyu, Y. Fu, X. Hu, and F. Li, "Coordinated microgrid frequency regulation based on dfig variable coefficient using virtual inertia and primary frequency control," *IEEE Trans. Energy Convers.*, vol. 31, no. 3, pp. 833–845, Sep. 2016.

[4] J. Ma, Y. Qiu, Y. Li, W. Zhang, Z. Song, and J. S. Thorp, "Research on the impact of DFIG virtual inertia control on power system small-signal stability considering the phase-locked loop," *IEEE Trans. Power Syst.*, vol. 32, no. 3, pp. 2094–2105, May 2017.

[5] S. D'Arco and J. A. Suul, "Virtual synchronous machines—Classification of implementations and analysis of equivalence to droop controllers for microgrids," in *Proc. IEEE Grenoble PowerTech*, Grenoble, France, Jun. 2013, pp. 1–7.

[6] H. Bevrani, T. Ise, and Y. Miura, "Virtual synchronous generators: A survey and new perspectives," *Int. J. Electr. Power Energy Syst.*, vol. 54, pp. 244–254, Jan. 2014.

[7] Q.-C. Zhong, Z. Ma, W.-L. Ming, and G. C. Konstantopoulos, "Grid-friendly wind power systems based on the synchronverter technology," *Energy Convers Manage.*, vol. 89, pp. 719–726 Jan. 2015.

[8] J. Liu, Y. Miura, and T. Ise, "Comparison of dynamic characteristics between virtual synchronous generator and droop control in inverter-based distributed generators," *IEEE Trans. Smart Grid*, vol. 31, no. 5, pp. 3600–3611, May 2016.

[9] S. M. Ashabani and Y. A. R. I. Mohamed, "A flexible control strategy for grid-connected and islanded microgrids with enhanced stability using nonlinear microgrid stabilizer," *IEEE Trans. Smart Grid*, vol. 3, no. 3, pp. 1291–1301, Sep. 2012.

[10] H.-P. Beck and R. Hesse, "Virtual synchronous machine," in *Proc. 9th Int. Conf. Elect. Power Qual. Utilisation*, Barcelona, Spain, Oct. 2007, pp. 1–6.

[11] K. Visscher and S. W. H. De Haan, "Virtual synchronous machines (VSG's) for frequency stabilisation in future grids with a significant share of decentralized generation," in *Proc. CIRED Seminar SmartGrids Distrib. (IET-CIRED)*, Frankfurt, Germany, Jun. 2008, pp. 1–4.

[12] J. Liu, Y. Miura, H. Bevrani, and T. Ise, "Enhanced virtual synchronous generator control for parallel inverters in microgrids," *IEEE Trans. Smart Grid*, vol. 8, no. 5, pp. 2268–2277, Sep. 2017.

[13] K. Lin, F. Xiao, G. Jie, C. Hou, and R. Wang, "Control strategy for inverter parallel and parallel with synchronous generator based on virtual synchronous generator theory," in *Proc. 36th Chin. Control Conf.*, Dalian, China, Jul. 2007, pp. 6453–6459.
[14] J. Fang, Y. Tang, H. Li, and X. Li, "A battery/ultracapacitor hybrid energy storage system for implementing the power management of virtual synchronous generators," *IEEE Trans. Power Electron.*, vol. 33, no. 4, pp. 2820–2824, Apr. 2017.
[15] Y. Ma, W. Cao, L. F. Yang, F. Wang, and L. M. Tolbert, "Virtual synchronous generator control of full converter wind turbines with short-term energy storage," *IEEE Trans. Ind. Electron.*, vol. 64, no. 11, pp. 8821–8831, Nov. 2017.
[16] M. Ashabani, Y. A.-R. I. Mohamed, "Novel comprehensive control framework for incorporating VSCs to smart power grids using bidirectional synchronous-VSC," *IEEE Trans. Power Syst.*, vol. 29, no. 2, pp. 943–957, Mar. 2013.
[17] T. Shintai, Y. Miura, and T. Ise, "Oscillation damping of a distributed generator using a virtual synchronous generator," *IEEE Trans. Power Del.*, vol. 29, no. 2, pp. 668–676, Apr. 2014.
[18] J. Alipoor, Y. Miura, and T. Ise, "Power system stabilization using virtual synchronous generator with alternating moment of inertia," *IEEE J. Emerg. Sel. Topics Power Electron.*, vol. 3, no. 2, pp. 451–458, Jun. 2015.
[19] M. Ashabani and Y. A.-R. I. Mohamed, "Integrating VSCs to weak grids by nonlinear power damping controller with self-synchronization capability," *IEEE Trans. Power Syst.*, vol. 29, no. 2, pp. 805–814, Mar. 2014.
[20] W. Wu *et al.*, "A virtual inertia control strategy for DC microgrids analogized with virtual synchronous machines," *IEEE Trans. Ind. Electron.*, vol. 64, no. 7, pp. 6005–6016, Jul. 2016.
[21] K. Shi *et al.*, "Grid-connected dual stator-winding induction generator wind power system for wide wind speed ranges," *J. Power Electron.*, vol. 16, no. 4, pp. 1455–1468, 2016.

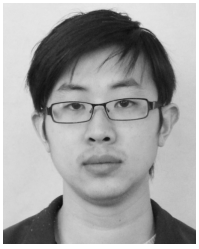

KAI SHI was born in Suzhou, China, in 1980. He received the B.S. degree in automation and the M.S. degree in power electronic and power transmission from Jiangsu University, Zhenjiang, China, in 2002 and 2005, respectively, and the Ph.D. degree in power electronic and power transmission from the Nanjing University of Aeronautics and Astronautics, Nanjing, China, in 2012. Since 2002, he has been with the School of Electrical and Information Engineering, Jiangsu University, where he has been an Assistant Professor since 2013. His current research interests include wind power generator control, grid-connected control, and control strategies of low-voltage ride through.

HAIHAN YE was born in Changzhou, China, in 1994. He received the B.S. degree in electrical engineering from the Wanfang Technology College, Henan Polytechnic University, Jiaozuo, China, in 2016. He is currently pursuing the Degree with the School of Electrical and Information Engineering, Jiangsu University, Zhenjiang, China. His research interests include the novel control technology of wind turbines.

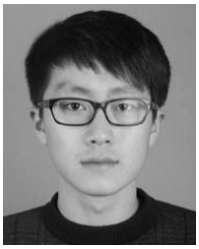

WENTAO SONG was born in Lianyungang, China, in 1995. He received the B.S. degree in electrical engineering from the Jiangsu University of Science and Technology, Zhenjiang, China, in 2017. He is currently pursuing the Degree with the School of Electrical and Information Engineering, Jiangsu University, Zhenjiang. His research interests include the novel control strategies of LVRT.

GUANGLEI ZHOU was born in Linyi, China, in 1994. He received the B.S. degree in electrical engineering from the Jiangsu University of Science and Technology, Zhenjiang, China, in 2017. He is currently pursuing the Degree with the School of Electrical and Information Engineering, Jiangsu University, Zhenjiang. His research interests include the islanding detection of inverter.